LANGMUIR

pubs.acs.org/Langmuir Article

Enhancing mRNA Interactions by Engineering the Arc Protein with Nucleocapsid Domain

Published as part of Langmuir special issue "2025 Pioneers in Applied and Fundamental Interfacial Chemistry: Shaoyi Jiang".

Vaibhav Upadhayay, Wenchao Gu,* and Qiuming Yu*

Cite This: *Langmuir* 2024, 40, 23473−23482 Read Online

ACCESS | Metrics & More | Article Recommendations | Supporting Information

ABSTRACT: Activity-regulated cytoskeleton-associated protein (Arc) forms virus-like capsids for mRNA transport between neurons. Unlike HIV-1 Group-specific Antigen (Gag), which uses its Nucleocapsid (NC) domain to bind HIV-1 genomic mRNA, mammalian Arc lacks the NC domain, and their direct mRNA binding interactions remain underexplored. This study examined rat Arc's binding to rat Arc 5′ UTR (A5U), HIV-1 5′ UTR (H5U), and GFP mRNAs, revealing weak binding with no significant preference. Adding the HIV-1 NC domain to rArc's C-terminus significantly improved binding to H5U, while also showing substantial binding to A5U at about 60% of its H5U level and exhibiting twice the affinity for A5U over GFP mRNA. Importantly, rArc-NC binds 3.4 times more A5U and H5U than GST-NC, indicating that rArc NTD-CA aids mRNA binding by HIV-1 NC. These findings suggest a conserved Gag protein−mRNA interaction mechanism, highlighting the potential for developing mRNA delivery systems that combine endogenous Gag NTD-CA with retroviral NC and UTRs.

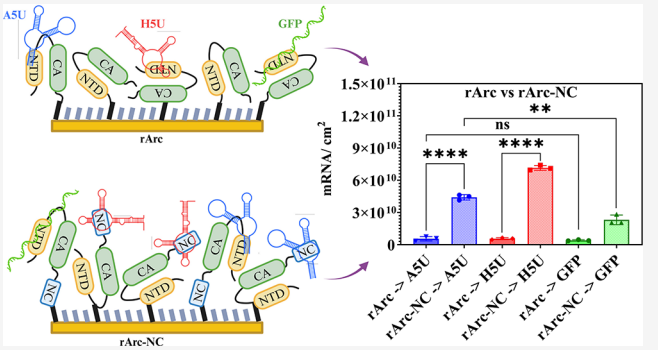

INTRODUCTION

The mammalian genome contains numerous protein-coding genes originally derived from sequences encoded by transposons[1] or retroviruses[2] that have been domesticated to restrict their function and repurpose these transposable elements as a genetic resource for novel purposes.[3] Interestingly, many of these transposon-derived genes are active in the brain.[4] While their specific molecular functions are often unclear, a few have gained scientific attention recently. One such example is the activity-regulated cytoskeleton-associated protein (Arc), which shares biochemical properties with retroviral/retrotransposon Gag proteins.[5,6] Arc is crucial for promoting synaptic plasticity and memory formation,[7] and its dysfunctions are associated with various neurological and neurodevelopmental disorders.[8−11] The retroviral-like properties of Arc include the ability to self-assemble into oligomeric particles resembling retrovirus capsids to encapsulate mRNA. These Arc capsids are released from neurons in extracellular vesicles (EVs) and facilitate the transfer of Arc mRNA to new target cells, where it can undergo activity-dependent translation in the mammalian brain.[12]

HIV-1 is one of the most extensively studied retroviral gag proteins. It consists of three major protein domains: matrix (MA), capsid (CA), and nucleocapsid (NC). The HIV-1 MA domain features a conserved cluster of highly basic amino acids that interact with acidic phospholipids, mediating Gag-membrane binding. Besides acidic phospholipids, the highly basic MA domain also binds to RNA. The CA domain primarily drives capsid formation, promoting protein−protein interactions via dimer, trimer, and hexamer interfaces. The NC domain of HIV-1 Gag is characterized by two zinc finger-like motifs flanked by highly basic sequences, recognizing the packaging signal in the viral genomic mRNA, which promotes selective viral genome packaging.[13−16] Studies have also shown that the NC domain alone is not sufficient for the encapsulation of the HIV-1 genomic mRNA but relies on the structural integrity of the CA domain lattice.[17] Mammalian Arc (mArc) proteins, gag homologues, contain the N-terminal Domain (NTD) and C-terminal CA domains but lack the NC domain and zinc fingers.[12,18] Despite missing the NC domain, recombinantly purified mArc proteins can still encapsulate

Received: August 12, 2024
Revised: October 3, 2024
Accepted: October 10, 2024
Published: October 21, 2024

https://doi.org/10.1021/acs.langmuir.4c03151
Langmuir 2024, 40, 23473−23482

mRNAs.[12,19] Recent findings indicate that mArc NTD has a positive patch of residues, termed an oligomerization motif, which may bind mRNAs through ionic interactions during capsid assembly inside cells or in solution.[19]

Interest in using endogenous capsid-forming proteins as drug carriers is growing due to their potential to deliver therapeutic mRNAs with high specificity and efficiency. However, a deeper understanding of the mechanisms behind the mRNA loading by these proteins is essential. An mRNA consists of a protein-coding open reading frame (ORF) flanked by two noncoding regions: the 5′ untranslated region (5′ UTR) at the beginning and the 3′ untranslated region (3′ UTR) at the end.[20] The 5′ UTR regulates mRNA translation into proteins, affecting the molecule's stability, localization, and translation. The 3′ UTR primarily regulates mRNA localization, stability, and translation.[21] Additionally, the UTRs of Gag proteins play a crucial role in mRNA encapsulation during the capsid assembly. HIV-1 gag selectively encapsulates genomic mRNA through specific interactions between the psi (ψ) signaling element in the HIV-1 5′ UTR and the NC domain's zinc fingers.[16,22−24] Unlike its mammalian orthologs, Drosophila Arc (dArc1) has an NC domain, and without its 3′ UTR, it shows low mRNA transduction efficiency and little cargo specificity.[25] Similarly, the encapsulation selectivity and mRNA delivery efficiency of Paternally Expressed Gene 10 (PEG10), which also has an NC domain, improve when the mRNA cargo is flanked by its 5′ and 3′ UTRs.[26] These highlight the crucial role of UTRs in Gag-NC proteins' capsid assembly. However, mArc lacking the NC domain can also encapsulate non-UTR mRNAs and form capsids in solution.[12,19] A recent study suggests that, although the rat Arc 5′ UTR enhances rat Arc capsid stability, which contributes to efficient encapsulation and transfer of mRNA both *in vitro* and *in vivo*, the system lacks specificity in selecting cargo for loading.[27] Overall, these findings highlight gaps in our understanding of endogenous Gag-mRNA interactions, which are crucial for the design of future endogenous retrovirus-like mRNA carriers.

In this work, we investigated fundamental protein−mRNA interactions in a cell-free environment, devoid of cellular components essential for capsid formation and mRNA encapsulation. Given the critical role of UTRs and NC domains in Gag protein capsid assembly and noting the absence of an NC domain in mammalian Arc proteins, we first examined the rat Arc (rArc) protein binding with two UTR sequences, rArc 5′ UTR (A5U) and HIV-1 5′UTR (H5U), as well as a non-UTR GFP ORF mRNA. Results obtained from both direct binding and sandwich assays showed no significant difference in rArc protein's binding to UTR and non-UTR mRNAs, suggesting that direct mRNA binding to rArc is primarily electrostatic via its NT domain. Subsequently, we modified the C-terminus of wild-type rArc, by adding the HIV-1 NC to evaluate its effect on mRNA binding. The engineered rArc-NC demonstrated significantly enhanced binding to H5U and A5U, with a 13-fold and 8-fold increase, respectively, compared to rArc. Additionally, rArc-NC exhibited nearly twice the binding affinity for A5U compared to GFP ORF mRNA, likely due to secondary structural similarity between A5U and H5U. This highlights the potential of rArc-NC as an endogenous virus-like mRNA carrier combining Gag NTD-CA with NC and UTR+ cargo mRNAs. Importantly, rArc-NC binds both A5U and H5U significantly more efficiently than GST-NC, suggesting that rArc's NT domain may facilitate electrostatic interactions with mRNAs while the CA lattice stabilizes these interactions, in addition to the direct binding by NC. These findings highlight again the potential for developing mRNA nanocarriers that integrate the capsid structure of endogenous Gag MA-CA domains with the binding specificity of retroviral NC and UTRs. Overall, this work offers insights into Gag-mRNA interactions and highlights potential protein engineering enhancements to improve the specificity and efficiency of endogenous virus-like mRNA delivery systems.

MATERIALS AND METHODS

Chemicals and Reagents. Oligo ethylene glycol (EG) alkanethiolates HS−$(CH_2)_{11}$−$(OC_2H_4)_4$−OH and HS−$(CH_2)_{11}$−$(OC_2H_4)_6$−OCH_2−COOH were purchased from ProChimia Surfaces (Gdynia, Poland). *N*-Hydroxysuccinimide (NHS), Tris base, glycerol, Tween-20, NuPAGE 4−12% Bis-Tris Mini Protein Gels, NuPAGE LDS Sample Buffer (4X), Pierce Protease Inhibitor Mini Tablets, Pierce Glutathione Agarose, SuperBlock Blocking Buffer, fluorescent secondary antibody (Alexa Fluor 647 goat antirabbit), Luria−Bertani (LB) broth, sodium chloride (≥99.0%), absolute ethanol (200-proof), Ampicillin sodium salt, and Pierce 660 nm Protein Assay Reagent were purchased from ThermoFisher Scientific (Waltham, MA). N-(3-(Dimethylamino)propyl)-N′-ethylcarbodiimide hydrochloride (EDC), HEPES, 2-mercaptoethanol (2-ME), Triton X-100, and magnesium chloride (≥99.0%) were purchased from Millipore Sigma (Burlington, MA). Ethanolamine hydrochloride (≥98.0%) was purchased from TCI America (Portland, OR). Nuclease and endotoxin-free molecular biology grade water was purchased from Neta Scientific (Marlton, NJ). Sodium acetate (99%) was purchased from BeanTown Chemical (Hudson, NH). PTFE 0.45 μm filters (25 mm) were purchased from Cole-Parmer (Vernon Hills, IL). Stable and BL21 competent *E. coli* cells, restriction enzymes (BamH1, Xho1, Apa1), DNA polymerase master mix (Phusion Hot Start Flex 2X Master Mix), Gibson Assembly Master Mix, HiScribe T7 mRNA Kit with CleanCap Reagent AG, and Monarch RNA Cleanup Kit were purchased from New England BioLabs (Ipswich, MA). Terrific Broth was purchased from Research Product International (Mt. Prospect, IL). Isopropyl β-D-1-thiogalactopyranoside (IPTG), reduced glutathione, dithiothreitol (DTT), and benzonase nuclease were purchased from Sigma-Aldrich (St. Louis, MO). PreScission protease was purchased from GenScript (Piscataway, NJ), and gravity flow columns were purchased from Marvelgent Biosciences (Canton, MA). The primary antibody (rabbit polyclonal anti-Arc) was purchased from Synaptic Systems (Göttingen, Germany). The Nucleospin Gel and PCR Clean-up Kit and Wizard Plus SV Minipreps DNA Purification Systems were purchased from Macherey-Nagel (Allentown, PA) and Promega Corporation (Madison, WI), respectively.

Plasmids Cloning. A rArc plasmid (pGEX-6p1-GST-ArcFL, #119877), GFP plasmid (pcDNA3-EGFP, #13031), HIV-1 Gag plasmid (pMET-GAG-HRAS, #80604), and HIV-1 pNL4-3 vector plasmid (pNL4-3 envFS eGFP gag2xFS, #101341) were purchased from Addgene (Watertown, MA). The A5U-GFP plasmid (pcDNA3-A5U-GFP) was provided by Dr. Wenchao Gu. The GST-NC protein construct was produced by PCR (primer sets in Table S3) amplifying the HIV-1 NC domain sequence from the HIV-1 Gag plasmid and ligating it into the BamH1 and Xho1 sites of the pGEX-6p1 backbone via Gibson assembly. rArc-NC was generated by Gibson assembly of PCR-amplified (primer sets in Table S3) rArc and NC fragments with the BamH1 and Xho1 linearized pGEX-6p1 vector. The H5U mRNA construct was produced by Gibson assembly of the PCR-amplified (primer sets in Table S3) H5U fragment from the HIV-1 pNL4-3 vector plasmid with the BamH1 and Apa1 linearized pcDNA3 vector. These plasmids were transformed into NEB Stable *E. coli* cells, and individual colonies were screened by full plasmid sequencing at Eurofins Genomics or PlasmidSaurus.

https://doi.org/10.1021/acs.langmuir.4c03151
Langmuir 2024, 40, 23473−23482

Protein Purification. The plasmids pGEX-6p1-GST-ArcFL, pGEX-6p1-GST-NC, and pGEX-6p1-GST-ArcFL-NC were transformed into *E. coli* BL21 competent cells and spread on LB agar plates containing ampicillin. The plates were incubated overnight at 37 °C. A single colony was picked to initiate starter cultures for protein expression and grown overnight at 37 °C in LB medium with ampicillin. These starter cultures were then used to inoculate 500 mL of 2X TB medium supplemented with ampicillin, 5 mM HEPES, and 2 mM $MgCl_2$. The cultures were grown at 37 °C and 250 rpm until the OD600 reached 0.5−0.7, followed by induction with 0.5 mM IPTG and incubation at 21 °C and 250 rpm for 18−20 h. Cultures were harvested by centrifugation at 6000*g* for 15 min at 4 °C, and the resulting cell pellets were flash-frozen using liquid nitrogen. For lysis, the pellets were resuspended in 20 mL of lysis buffer (50 mM Tris, 100 mM NaCl, 5% glycerol, 1 mM DTT, 0.1% Triton X-100, 2 mM $MgCl_2$, pH 8.0) along with two protease inhibitor tablets and 2500 units of Benzonase Nuclease. The cells were lysed by sonication (10 pulses of 30 s on and 90 s off at a 60% duty cycle), and the debris was pelleted by centrifugation at 22 000*g* for 1 h. The cleared lysates were incubated with GST agarose affinity resin overnight at 4 °C. The resin-bound protein was washed four times on a gravity flow column using a wash buffer (50 mM Tris, 100 mM NaCl, 1 mM EDTA, 1 mM DTT, 0.1% Triton X-100, 5% glycerol, pH 8.0). The GST-NC protein was eluted with GST elution buffer (50 mM Tris, 50 mM NaCl, and 10 mM reduced glutathione, pH 8.0). For the rArc and rArc-NC constructs, the resin-bound protein was re-equilibrated in elution buffer (containing 100 mM NaCl, 50 mM Tris, 1 mM EDTA, 1 mM DTT, pH 8.0) and cleaved on-resin overnight at 4 °C using PreScission Protease. The cleaved rArc and rArc-NC proteins were eluted, while the GST protein bound to the resin was subsequently eluted with the GST elution buffer. The purity of the proteins was verified by SDS-PAGE and Western blot. Protein concentrations were measured using a BioTek Cytation 7 Imager and a Pierce 660 nm Protein Assay Kit.

Western Blot Analysis. 100 ng of purified rArc and rArc-NC proteins were mixed with NuPAGE LDS Sample Buffer (4X) and 10% 2-ME, then incubated at 90 °C for 10 min. The samples were loaded onto NuPAGE 4−12% Bis-Tris Mini Protein gels and run at 200 V for 30 min to separate the proteins. Proteins were transferred to a PVDF membrane by using the iBlot2 system (ThermoFisher Scientific). Membranes were blocked with SuperBlock Blocking Buffer for 1 h at room temperature, followed by overnight incubation at 4 °C with 0.5 μg/mL Arc primary antibody in SuperBlock Blocking Buffer. After five washes with 1X PBST (1X PBS with 0.05% Tween-20), membranes were incubated with 0.4 μg/mL fluorescent secondary antibody in SuperBlock Blocking Buffer for 1 h at RT, washed five times with 1X PBST, and imaged using the Azure Biosystems 300 Imager.

***In Vitro* Transcription of mRNA.** The plasmids encoding A5U (pcDNA3-A5U-GFP), H5U (pcDNA3-H5U), and GFP (pcDNA-EGFP) mRNAs were linearized by PCR (primer sets in Table S3) and purified using the Macharey-Nagel Nucleospin Gel and PCR Clean-up Kit. Primers were designed with the forward primer upstream of the T7 promoter (all mRNAs) and the reverse primer, adding a 120 bp polyA tail to the GFP mRNA. The A5U and H5U mRNAs did not have a polyA tail. mRNA was synthesized with the HiScribe T7 mRNA Kit with CleanCap Reagent AG, following the manufacturer's protocol. After 2 h of incubation at 37 °C, 30 μL of water and 2 μL of DNase I were added to the reaction mixture and incubated for 1 h at 37 °C. The mRNA was then purified using the Monarch RNA Cleanup Kit as per the manufacturer's protocol. mRNA quality was verified by gel electrophoresis and fragment bioanalyzer, and mRNA concentration was measured using a BioTek Cytation 7 Imager.

SPR Biosensor. A six-channel SPR biosensor developed at the Institute of Photonics and Electronics, Prague, Czech Republic, was used in this study.[40] This biosensor, with temperature stabilization, utilizes wavelength spectroscopy of surface plasmons. It features a dispersionless microfluidic system that delivers the sample analyte directly to the SPR chip surface using a two-pump system, eliminating inter- and intradispersion effects. Light is collimated and polarized in the sensor head before it reaches the SPR coupling prism. The reflected light is collected and directed to a six-channel spectrograph. SPR gold chips were prepared by coating glass slides with a thin layer of titanium (1−2 nm) and gold (48 nm) via electron-beam evaporation at the Cornell NanoScale Facility (CNF). The SPR chip is coupled with the prism by using immersion oil to match the refractive index, preventing irrelevant signals. A flow cell with six separate chambers, each about 80 μm deep, confines the sample during the experiments. A peristaltic pump delivers the liquid sample to the flow cell and sensor surface. The sensor has a temperature controller (ILX Lightwave, LDT-5525) to maintain temperatures between 5 and 40 °C. In this study, a 1 nm SPR wavelength shift corresponded to a change in protein surface coverage of 17 ng/cm^2,[41] which was used to calibrate the surface coverage of bound protein.

Surface Functionalization and Protein Immobilization. Gold-coated SPR chips were rinsed with Milli-Q water and absolute ethanol and then dried with nitrogen. The gold surface was treated with oxygen plasma at medium RF power on a Harrick Plasma Cleaner for 5 min, rinsed again with Milli-Q water and absolute ethanol, and dried with nitrogen. The chips were immersed in a 0.2 mM ethanolic solution of OEG_4OH and OEG_6COOH thiols in a 7:3 ratio for 16−20 h. After rinsing with ethanol and Milli-Q water and drying with nitrogen, the chips were mounted on the SPR sensor using immersion oil to match the refractive index of the prism. All SPR experiments were performed at 25 °C with a baseline stability of 0.01 °C. Protein immobilization was conducted in real-time. A baseline was established under Milli-Q water at 20 μL/min. Carboxylate groups from OEG_6COOH thiols were activated with a mixture of NHS (20 mM) and EDC (80 mM) in Milli-Q water for 10 min at 5 μL/min, followed by a Milli-Q wash at 20 μL/min. Sodium acetate buffer (SA-10, pH 5.0) was introduced, and protein solutions (50−100 μg/mL GST, GST-NC, rArc, and rArc-NC in SA-10, pH 5.0) were injected at 20 μL/min until the surface had ∼(3.3−3.5) × 10^{12} proteins/cm^2. The protein density calculation is provided in Note S1 and Table S1, showing the theoretical estimate for the total number of bound proteins/cm^2 based on a reference protein of MW 60 kDa. The immobilized surface was washed with SA-10 for 3 min, followed by a 2 min exposure to PBS with 0.5 M NaCl (PBS-Na) to remove noncovalently bound proteins. A short SA-10 wash followed. Residual unreacted NHS groups were deactivated by injecting 1 M ethanolamine buffer (pH 8.0) for 10 min at a rate of 20 μL/min. SA-10 buffer was injected again to establish the final protein immobilization levels (Figure S4).

Detection of mRNA Bound to Proteins. Tris50 buffer (50 mM Tris, pH 7) was used for the detection of mRNA bound to immobilized proteins. 100 nM A5U, H5U, and GFP ORF mRNA samples in Tris50 were flowed over protein-functionalized and reference (GST immobilized) surfaces for 13 min at 20 μL/min. After detection, the Tris50 buffer was flowed for at least 15 min at 20 μL/min to re-establish the baseline. The final detection levels of mRNAs bound to proteins were measured by the wavelength shift difference between buffer baselines before sample injection and after Tris50 buffer washing. To account for molecular weight differences among the mRNAs, the wavelength shifts were converted to the number of mRNA molecules per square centimeter of the SPR chip surface. The calculation is provided in Note S2 and Table S2, showing the theoretical estimate for the total number of protein-bound mRNA/cm^2 based on a reference protein of MW 60 kDa.

Sandwich Assays. For the sandwich assays, 100 nM A5U, H5U, and GFP ORF mRNAs were flowed over the surface functionalized with either GST-NC or rArc-NC as described above. After mRNA detection and baseline establishment by Tris50 buffer, 200 nM rArc protein was flowed over the mRNA for 8 min at 20 μL/min. This was followed by flowing Tris50 for 10 min at a rate of 20 μL/min to reestablish the baseline. The final detection levels of rArc protein captured by bound mRNAs were determined by the wavelength shift difference between the buffer baselines before and after Tris50 buffer washing. The number of rArc proteins captured by bound mRNAs per square centimeter of the SPR chip surface was then calculated as previously described. Similarly, the number of mRNA proteins bound to either GST-NC or rArc-NC was calculated as described earlier.

https://doi.org/10.1021/acs.langmuir.4c03151
Langmuir 2024, 40, 23473−23482

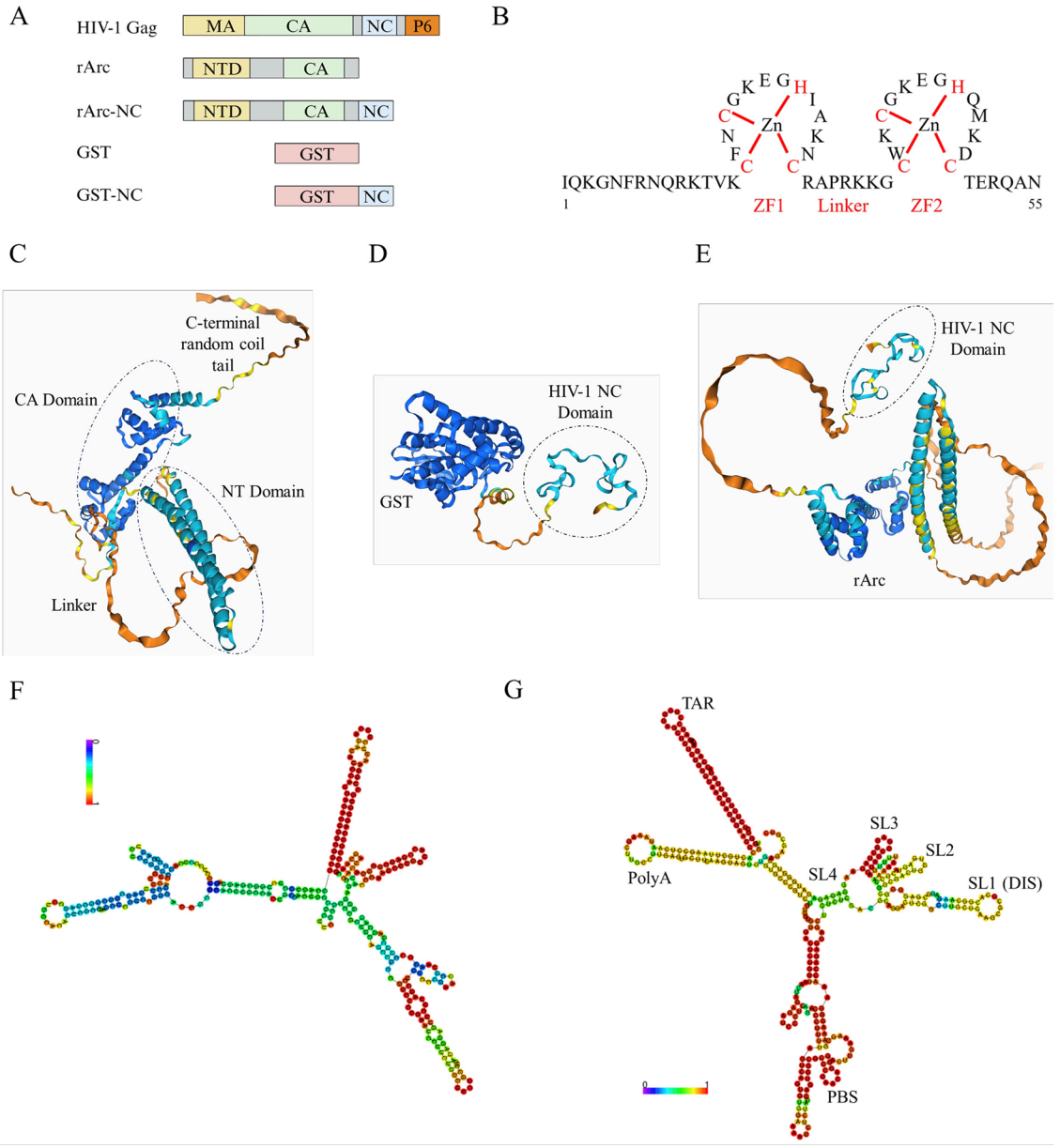

Figure 1. (A) Domain architecture comparison of proteins used in this study with HIV-1 Gag. (B) The amino acid sequence of the HIV-1 NC domain featuring two zinc fingers, ZF1 and ZF2, linked by a basic region. AlphaFold-predicted secondary structures of (C) rArc with highlighted protein domains, (D) the HIV-1 NC domain with an N-terminal GST fusion tag (GST-NC), and (E) the engineered rArc protein with an HIV-1 NC domain (rArc-NC), displaying the HIV-1 NC domain appended to the C-terminal random coil tail of rArc. Vienna RNAfold-predicted secondary structures of (F) A5U and (G) H5U with main stem-loops highlighted. Scale-bar indicates base-pair probabilities.

The ratio of these two values provided the number of rArc proteins captured by a single-bound mRNA molecule.

Statistical Analysis. Experimental data are shown as mean ± standard deviation using bar graphs. Statistical analyses were performed using GraphPad Prism (version 10.0.2). Sample comparisons were made using the unpaired *t* test, where ns indicates $p > 0.05$, * indicates $p \leq 0.05$, ** indicates $p \leq 0.01$, *** indicates $p \leq 0.001$, and **** indicates $p \leq 0.0001$.

RESULTS AND DISCUSSION

Production of Recombinant GST, rArc, GST-NC, and rArc-NC Proteins. Figure 1A shows the domain architecture comparison between the proteins used in this study and those in HIV-1 Gag. The study utilized GST, wildtype rArc, the HIV-1 NC domain with an N-terminal GST tag (GST-NC), and an engineered rArc protein with a C-terminal HIV-1 NC domain after the random coil tail of rArc (rArc-NC). This rArc-NC design allowed the random coil tail of rArc to serve as a linker, ensuring the independent folding of rArc and NC proteins without disrupting their secondary structures. This was confirmed by the structural model of the engineered rArc-NC protein, built using AlphaFold2[28] under the colabfold framework.[29] The secondary structure indicated that the rArc and NC fragments folded independently, as shown in Figure 1E compared to wildtype rArc and GST-NC in Figure 1C and D, respectively. To maximize the soluble protein yield, a pGEX expression vector was used, adding a GST fusion tag to the N-terminus of each protein. Recombinant fusion proteins were expressed in bacteria via IPTG induction. SDS-PAGE analysis confirmed the presence of rArc (45.33 kDa), GST-NC (34.08 kDa), and rArc-NC (53.01 kDa) in purified samples (Figure

https://doi.org/10.1021/acs.langmuir.4c03151
Langmuir 2024, 40, 23473−23482

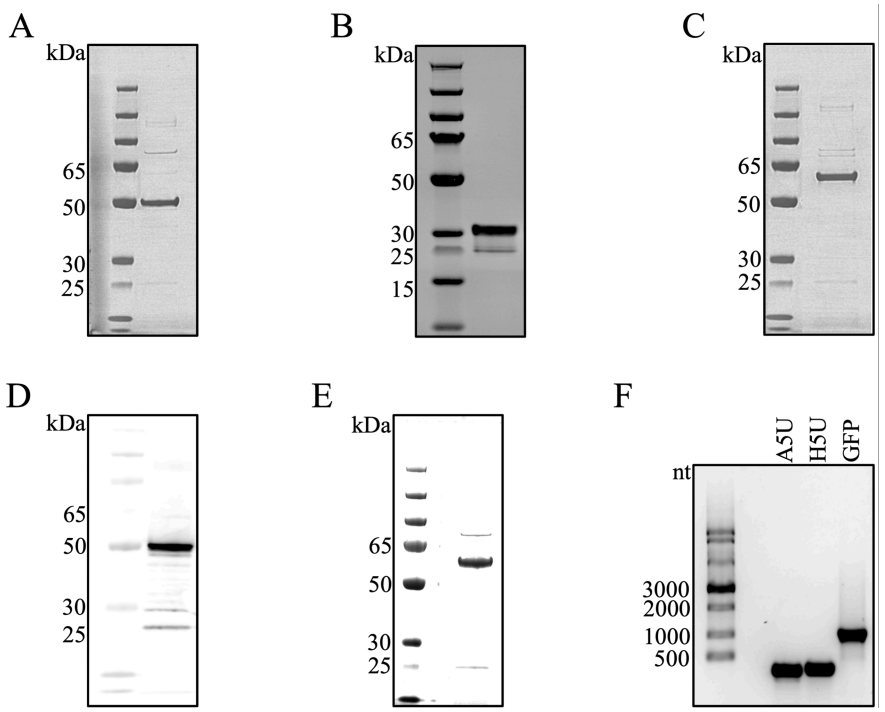

Figure 2. SDS-PAGE analysis of the purified recombinant (A) rArc, (B) GST-NC, and (C) rArc-NC proteins showing their size and purity. Western Blot analysis of the purified (D) rArc and (E) rArc-NC proteins. (F) Gel electrophoresis showing the size and quality of the *in vitro* transcribed A5U, H5U, and GFP mRNAs.

2A−C) with purities of approximately 90%, 85%, and 90%, respectively, as determined by ImageJ (Figure S1A−C). Additionally, Western Blotting using an anti-Arc polyclonal antibody verified the immunoreactivity of rArc and rArc-NC proteins (Figure 2D and E). The yields were approximately 1 mg for rArc and rArc-NC and 5 mg for GST-NC, per liter of bacterial culture. Proteins were stored at −80 °C with final protein concentrations between 200 and 300 μg/mL. The GST tag (26.43 kDa), eluted after rArc and rArc-NC, was analyzed by SDS-PAGE and found to be 100% pure (Figure S6A). It was stored under the same conditions as those of the other proteins.

***In Vitro* Transcription of A5U, H5U, and GFP mRNAs.** Two UTR mRNAs, rArc 5′UTR (A5U) and HIV-1 5′UTR (H5U), along with a non-UTR GFP ORF mRNA with a polyA tail were utilized in this study. The molecular weights of these mRNAs were 106.89, 121.69, and 382.95 kDa, respectively. They were synthesized via *in vitro* transcription (IVT) using T7 RNA polymerase, with linearized plasmids serving as templates. RNA quality and size were verified through gel electrophoresis, showing prominent bands corresponding to A5U (334 bases), H5U (396 bases), and GFP (1186 bases; Figure 2F). Further size and integrity confirmations were obtained using a fragment BioAnalyzer (Figure S2A−C). Spectrophotometric analysis yielded A_{260}/A_{280} ratios of >2, indicating minimal protein or DNA contamination. The synthesized mRNAs had concentrations of approximately 2 mg/mL and were stored at −80 °C without dilution.

Surface Plasmon Resonance (SPR) Biosensors for Cell-Free Protein−mRNA Binding. Cellular components like cell membrane[30−32] and tRNA[33,34] influence gag protein−mRNA interactions during capsid assembly. To isolate these effects and understand protein−mRNA binding in real-time, cell-free methods are crucial. Therefore, real-time cell-free protein−mRNA binding experiments were conducted using a custom-built six-channel SPR biosensor. Gold-coated SPR chips were functionalized with a low-fouling self-assembled monolayer (SAM) of the OEG_4OH/OEG_6COOH (OH/COOH) in a 7:3 ratio (Figure S3A). Proteins were immobilized via amine coupling with carbodiimide chemistry (Figure S3B and C). A detailed sensorgram of the immobilization process is shown in Figure S4A and B. The surface protein density for all proteins was standardized based on the surface density that ensured 100% surface coverage of rArc (Note S1). Table S1 lists the surface protein densities for the immobilized proteins (GST, rArc, GST-NC, and rArc-NC), with the GST surface serving as a reference for nonspecific interactions and baseline drift. To investigate the protein−mRNA binding interactions, mRNA samples were flowed through the protein-functionalized sensor surfaces (Figure 3A−C). The wavelength shifts in the SPR sensorgram after mRNA flow indicated successful protein−mRNA binding. The wavelength shifts, caused by changes in the local refractive index upon protein−mRNA binding, are proportional to the molecular weight of mRNA and were used to quantify the number of mRNA molecules per cm^2 binding to the proteins (Note S2 and Table S2).

Interaction of Wildtype rArc Protein with mRNAs. The NC domain in retroviruses is crucial for RNA encapsulation and maintaining capsid integrity as it specifically binds to the unique 5′ UTRs to package viral genomic RNA into capsids. Although rArc lacks the NC domain, it can form capsids with both its own UTR and non-UTR mRNA.[12,19,27] While including the A5U motif in cargo mRNA stabilizes rArc capsids, rArc does not preferentially load A5U-bearing mRNAs.[27] Overall, these findings suggest that unlike retroviral and drosophila proteins, the rArc protein may not selectively bind its UTRs. Using direct binding methods like SPR to

https://doi.org/10.1021/acs.langmuir.4c03151
Langmuir 2024, 40, 23473−23482

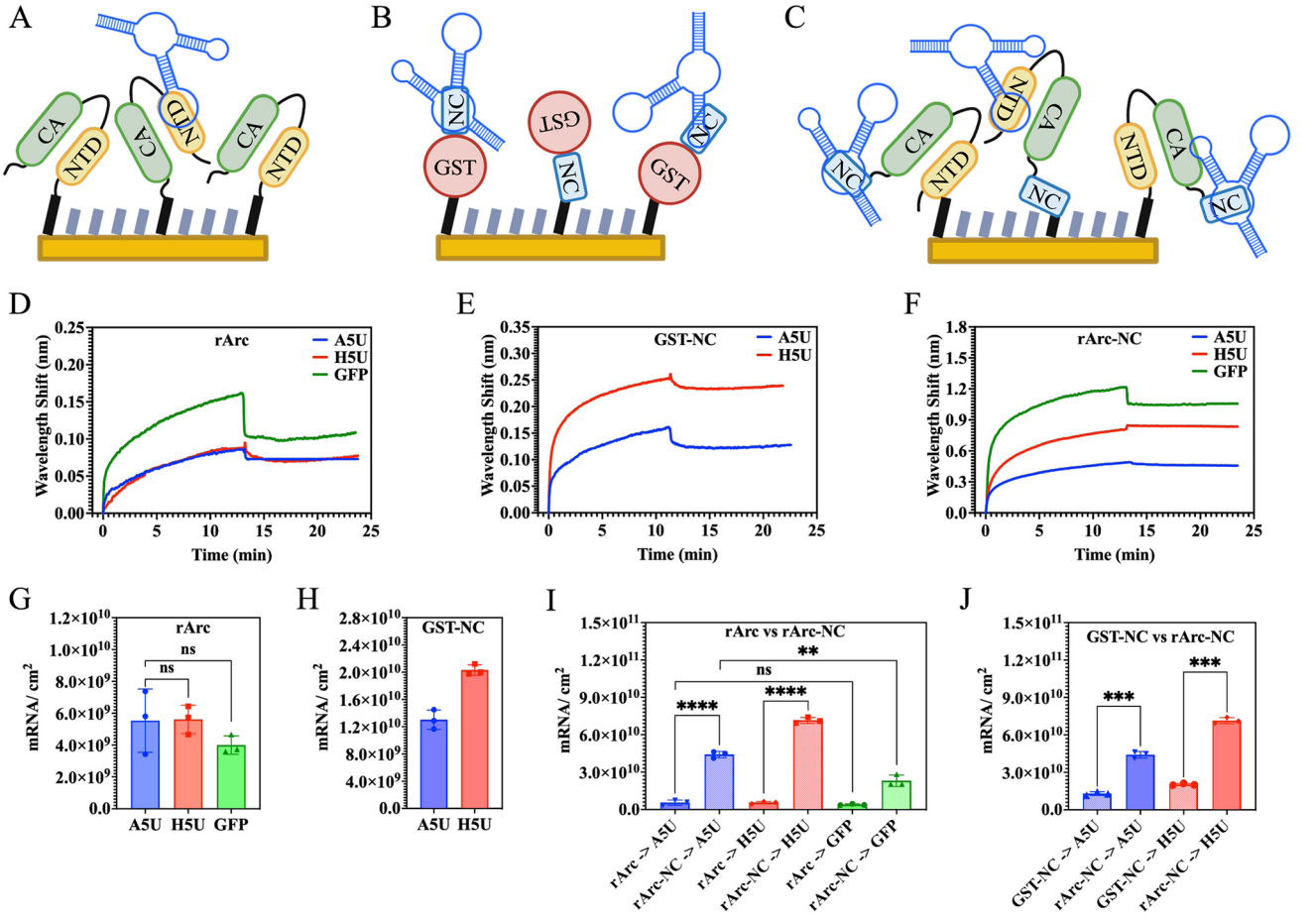

Figure 3. Schematic representation of SPR binding assays with A5U mRNA captured by (A) rArc, (B) GST-NC, and (C) rArc-NC proteins. Real-time SPR sensorgrams showing the capture of (D) 100 nM A5U, H5U, and GFP mRNAs by rArc, (E) 100 nM A5U and H5U mRNAs by GST-NC, and (F) 100 nM A5U, H5U, and GFP mRNAs by rArc-NC. Bar graph displaying the number of (G) A5U, H5U, and GFP mRNAs bound per cm^2 of the chip surface by rArc; (H) A5U and H5U mRNAs bound per cm^2 of the chip surface by GST-NC; and (I) A5U, H5U, and GFP mRNAs bound per cm^2 of the chip surface by rArc and rArc-NC. (J) Bar graph comparing the number of A5U and H5U mRNAs bound per cm^2 of the chip surface by GST-NC and rArc-NC. Samples were compared using an unpaired *t* test where ns represents a $p > 0.05$, * represents $p \leq 0.05$, ** represents $p \leq 0.01$, *** represents $p \leq 0.001$, and **** represents $p \leq 0.0001$.

assess rArc binding to UTR versus non-UTR mRNAs is crucial for understanding mRNA−protein binding mechanisms in retrotransposon capsids. Here, we used two 5′UTR mRNA motifs, A5U and H5U, and a non-UTR GFP ORF mRNA to assess how these mRNAs interact with the rArc protein in a cell-free environment. The SPR wavelength shifts indicated weak binding of the three mRNAs by rArc protein (Figure 3D), with no significant difference observed in the number of A5U, H5U, and GFP mRNAs bound (Figure 3G). These results demonstrate the critical role of the NC domain in effective and specific mRNA binding, suggesting that in its absence, the binding of mRNAs to surface-bound rArc proteins is not dependent on mRNA identity but is predominantly electrostatic, mediated by the NT domain.[19,35] The NT domain, which typically binds to the cell membrane during capsid assembly due to its positive charge, primarily binds to negatively charged mRNA in the absence of the cell membrane. To minimize potential mRNA degradation or loss of secondary structure, we conducted binding experiments with mRNA incubated with 3 mM Mg^{2+} at 4 °C before testing. Mg^{2+} ions stabilize mRNA by neutralizing the negatively charged phosphate backbone.[36−38] No differences were observed in rArc-mRNA binding with or without Mg^{2+} incubation (Figure S5A and B), supporting the authenticity of the results obtained. GST protein, with no known mRNA binding sites, was used as a reference in our assays. Assays on GST-functionalized surfaces showed negligible mRNA binding (Figure S6B,C), confirming that the interactions observed were specific to the rArc protein and not due to experimental artifacts. In conclusion, these results show that without an NC domain, rArc protein lacks strong or specific mRNA binding. This suggests a broader, less selective interaction mechanism during mammalian retrotransposon capsid assembly, indicating the need for further studies to enhance mRNA encapsulation for developing new mRNA drug delivery carriers based on mammalian Arc proteins.

Interaction of Engineered rArc Protein with mRNAs. The NC domain is a 55 amino acid sequence in the HIV-1 Gag polyprotein, containing two zinc finger-like motifs of the form Cys-X_2-Cys-X_4-His-X_4-Cys (X = variable amino acid), where three cysteines and one histidine bind to a Zn^{2+} ion. These zinc fingers are separated by a basic linker segment (Figure 1B).[16] The zinc fingers are involved in recognizing and encapsulating the HIV-1 genomic RNA through specific interactions with the psi signaling element in the H5U.[13,17] The psi element contains four stem-loop structures (SL1 through SL4, Figure

https://doi.org/10.1021/acs.langmuir.4c03151
Langmuir 2024, 40, 23473−23482

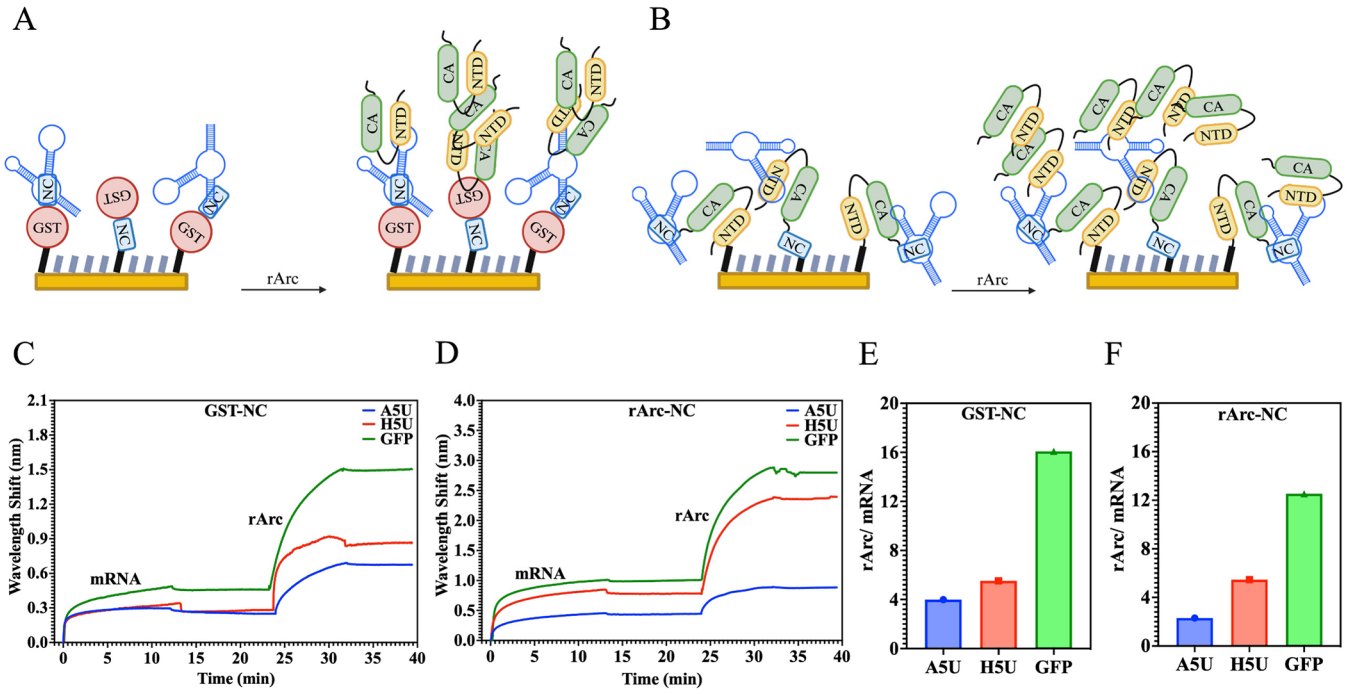

Figure 4. Schematic representation of sandwich assays with A5U mRNA captured by (A) immobilized GST-NC and (B) immobilized rArc-NC proteins followed by flowing free rArc proteins. Real-time sensorgrams showing the capture of A5U, H5U, and GFP mRNAs by (C) immobilized GST-NC and (D) immobilized rArc-NC proteins and the subsequent binding of free rArc to mRNAs. Bar graphs display the number of rArc proteins bound per A5U, H5U, and GFP mRNAs captured by (E) immobilized GST-NC and (F) immobilized rArc-NC.

1G) that aid in recognizing the HIV-1 genomic RNA.[16,22] To examine how the HIV-1 NC domain affects an exogenous Gag protein and alters its binding to mRNAs, we engineered rArc by adding the HIV-1 NC domain to its C-terminus. SPR binding assays using immobilized rArc-NC (engineered rArc) and A5U, H5U, and GFP mRNAs demonstrated enhanced mRNA binding compared to wildtype rArc. Notably, Figure 3F shows that the wavelength shifts of mRNAs binding to immobilized rArc-NC are approximately an order of magnitude higher than rArc (Figure 3D), indicating increased mRNA binding per cm^2 of the chip surface. Specifically, rArc-NC bound to H5U and A5U mRNAs approximately 13 and 8 times more effectively than did rArc. rArc-NC exhibited higher binding to H5U than to A5U and GFP mRNAs. It showed substantial binding to A5U at about 60% of its H5U level and twice the affinity for A5U over GFP mRNA (Figure 3I), highlighting its ability to differentiate between UTR and non-UTR mRNAs in a cell-free environment. Furthermore, despite both GST-NC and Arc-NC proteins having the same NC domain at their C-terminal ends, rArc-NC bound 3.4 times more mRNA (A5U and H5U) than GST-NC (Figure 3J). This underscores the influence of the partner protein; GST in GST-NC does not bind mRNA, while rArc in rArc-NC enhances mRNA binding through the NT domain. It demonstrates the collaborative nature of Gag protein domains in mRNA binding and highlights the potential of combining the endogenous Gag NTD-CA shell with the retroviral NC and UTRs for developing new mRNA drug carriers. Notably, the HIV-1 NC domain, purified with the GST tag intact (GST-NC), bound not only to H5U mRNA, as expected, but also to a significant amount of A5U mRNA (Figure 3E and H). This can be explained by the predicted secondary structures from Vienna RNAfold,[39] showing very similar stem-loops for A5U and H5U (Figure 1F and G), suggesting that the interaction of A5U with the NC domain may involve nonelectrostatic components. This finding suggests a potentially conserved RNA binding mechanism in both retroviral and retrotransposon Gag proteins influenced by UTR secondary structures. If the HIV-1 NC domain can effectively load A5U, other endogenous Gag homologous genes in mammalian cells might also be targeted for loading into Gag-NC capsids. Future *in vitro* and *in vivo* studies are needed to assess the specificity of mRNA drug loading, as delivering multiple gag genes along with an mRNA drug could complicate therapeutic applications.

Unlike retroviral Gag proteins or Drosophila Arc, mammalian Arc lacks an NC domain, which is critical for RNA binding and capsid assembly in retroviruses. However, our study reveals that rArc can still facilitate HIV-1 NC in loading the HIV 5′ UTR, indicating functional and structural parallels between rArc and retroviral Gag. Interestingly, rArc does not specifically or strongly bind to its own 5′ UTR, setting it apart from retroviruses. This raises compelling questions about how mammalian Arc has evolved to form capsid-like structures and interact with mRNA. Further studies are necessary to evaluate the specificity of mRNA drug loading via Gag proteins and investigate the potential of incorporating a Gag NC domain into human Arc. This modification could enhance mRNA binding and support functional capsid formation, offering promising prospects for drug delivery in humans.

Sandwich Assays with Free rArc Protein and Bound mRNAs. The direct binding assays demonstrated that immobilized rArc protein binds to both UTR and non-UTR mRNAs without distinction, raising critical questions about how free rArc protein interacts with these mRNAs in a cell-free environment. To address these questions, we performed sandwich assays with free rArc protein and bound mRNAs. In these sandwich assays, 100 nM A5U, H5U, and GFP mRNAs were first bound on surfaces with immobilized GST-

https://doi.org/10.1021/acs.langmuir.4c03151
Langmuir 2024, 40, 23473−23482

NC or rArc-NC proteins, followed by the addition of 200 nM free rArc protein to be captured by the bound mRNAs (Figure 4A and B). Since rArc protein was flowed over the immobilized GST-NC and rArc-NC surfaces, it could also interact with these proteins in addition to the mRNA bound to them. To account for protein−protein interactions in these sandwich assays, reference channels were used where the buffer was flowed instead of mRNA, followed by free rArc. The actual responses for mRNA and free rArc interactions were obtained by subtracting the reference channel responses from the analyte channel responses (Figure S7). Real-time sensorgrams in Figure 4C and D show the capture of A5U, H5U, and GFP mRNA by GST-NC and rArc-NC, respectively, and the subsequent interaction of free rArc proteins with the bound mRNAs. To allow a fair comparison despite different mRNA sizes and molecular weights, the number of rArc proteins captured by one molecule of A5U, H5U, and GFP mRNAs was calculated. Figure 4E and F show that the number of rArc proteins per mRNA follows the same trend for mRNAs bound to either GST-NC or rArc-NC: rArc/A5U < rArc/H5U < rArc/GFP. This trend aligns with the mRNA sizes, A5U < H5U < GFP, indicating that larger mRNAs, which carry more negative charge, bind more rArc molecules. This suggests that the interaction of rArc with mRNAs in the absence of cellular components is mainly electrostatic and independent of mRNA identity, like observations from direct binding assays. In conclusion, both immobilized and free rArc protein interacts with UTR and non-UTR mRNAs similarly in a cell-free environment.

CONCLUSIONS

In conclusion, this study explored protein−mRNA interactions in a cell-free system, specifically, focusing on the rat Arc (rArc) protein with and without the HIV-1 NC domain and their interactions with rArc 5′UTR (A5U), HIV-1 5′UTR (H5U), and non-UTR GFP ORF mRNAs. Wildtype rArc showed nonselective, mainly electrostatic mRNA binding, whereas the engineered rArc-NC had significantly improved interactions, especially with UTR mRNAs. These findings highlight the potential of using structural components from endogenous Gag NTD-CA domains, retroviral NC, and UTRs to create effective, virus-like mRNA delivery systems. This research lays the groundwork for designing endogenous capsid proteins, aiming to use the Arc protein as a gene therapy delivery vehicle.

ASSOCIATED CONTENT

Supporting Information

The Supporting Information is available free of charge at https://pubs.acs.org/doi/10.1021/acs.langmuir.4c03151.

Supplementary Figures, Notes, and Tables; ImageJ analysis of SDS-PAGE gel for purified proteins, BioAnalyzer fragment analysis of the *in vitro* transcribed mRNAs; schematic showing mixed self-assembled monolayer (SAM) formation and surface functionalization with rArc protein through amine coupling; sensorgram showing immobilization of GST and rArc proteins; estimation of protein surface coverage; estimation of mRNA/cm^2 from SPR wavelength shift; impact of Mg^{2+} on protein−mRNA binding; mRNA binding experiments on GST functionalized reference surfaces; sensorgram showing the real-time response of the reference, analyte, and the reference subtracted analyte channels for the sandwich assays; and primer sequences used in the study (PDF)

AUTHOR INFORMATION

Corresponding Authors

Wenchao Gu − *Meinig School of Biomedical Engineering, Cornell University, Ithaca, New York 14853, United States;* orcid.org/0000-0002-0967-1682; Email: wg246@cornell.edu

Qiuming Yu − *Robert Frederick Smith School of Chemical and Biomolecular Engineering, Cornell University, Ithaca, New York 14853, United States;* orcid.org/0000-0002-2401-4664; Email: qy10@cornell.edu

Author

Vaibhav Upadhayay − *Robert Frederick Smith School of Chemical and Biomolecular Engineering, Cornell University, Ithaca, New York 14853, United States*

Complete contact information is available at: https://pubs.acs.org/10.1021/acs.langmuir.4c03151

Author Contributions

V.U., W.G., and Q.Y. conceptualized the work. V.U. acquired the data. V.U. and Q.Y. performed the data analyses and the interpretation of the results. W.G. provided advice, support, and supervision. V.U. wrote the manuscript. V.U., W.G., and Q.Y. edited the manuscript.

Notes

The authors declare no competing financial interest.

ACKNOWLEDGMENTS

The authors gratefully acknowledge the financial support by the National Science Foundation (NSF; CBET-2247222). This work was performed in part at the Cornell NanoScale Facility, a member of the National Nanotechnology Coordinated Infrastructure (NNCI), which is supported by the NSF (Grant NNCI-2025233). The opinions, findings, conclusions, and recommendations expressed in this material are solely those of the authors and do not necessarily reflect the views of the NSF.

REFERENCES

(1) Feschotte, C.; Pritham, E. J. DNA Transposons and the Evolution of Eukaryotic Genomes. *Annu. Rev. Genet* **2007**, *41*, 331−368.

(2) Kaneko-Ishino, T.; Ishino, F. The Role of Genes Domesticated from LTR Retrotransposons and Retroviruses in Mammals. *Front Microbiol* **2012**, *3*, 262.

(3) Smit, A. F. Interspersed Repeats and Other Mementos of Transposable Elements in Mammalian Genomes. *Curr. Opin Genet Dev* **1999**, *9* (6), 657−663.

(4) Chesnokova, E.; Beletskiy, A.; Kolosov, P. The Role of Transposable Elements of the Human Genome in Neuronal Function and Pathology. *Int. J. Mol. Sci.* **2022**, *23* (10), 5847.

(5) Campillos, M.; Doerks, T.; Shah, P. K.; Bork, P. Computational Characterization of Multiple Gag-like Human Proteins. *Trends Genet* **2006**, *22* (11), 585−589.

(6) Zhang, W.; Wu, J.; Ward, M. D.; Yang, S.; Chuang, Y.-A.; Xiao, M.; Li, R.; Leahy, D. J.; Worley, P. F. Structural Basis of Arc Binding to Synaptic Proteins: Implications for Cognitive Disease. *Neuron* **2015**, *86* (2), 490−500.

(7) Chowdhury, S.; Shepherd, J. D.; Okuno, H.; Lyford, G.; Petralia, R. S.; Plath, N.; Kuhl, D.; Huganir, R. L.; Worley, P. F. Arc/Arg3.1

Interacts with the Endocytic Machinery to Regulate AMPA Receptor Trafficking. *Neuron* **2006**, *52* (3), 445−459.
(8) Wu, J.; Petralia, R. S.; Kurushima, H.; Patel, H.; Jung, M.; Volk, L.; Chowdhury, S.; Shepherd, J. D.; Dehoff, M.; Li, Y.; Kuhl, D.; Huganir, R. L.; Price, D. L.; Scannevin, R.; Troncoso, J. C.; Wong, P. C.; Worley, P. F. Arc/Arg3.1 Regulates an Endosomal Pathway Essential for Activity-Dependent β-Amyloid Generation. *Cell* **2011**, *147* (3), 615−628.
(9) Greer, P. L.; Hanayama, R.; Bloodgood, B. L.; Mardinly, A. R.; Lipton, D. M.; Flavell, S. W.; Kim, T.-K.; Griffith, E. C.; Waldon, Z.; Maehr, R.; Ploegh, H. L.; Chowdhury, S.; Worley, P. F.; Steen, J.; Greenberg, M. E. The Angelman Syndrome Protein Ube3A Regulates Synapse Development by Ubiquitinating Arc. *Cell* **2010**, *140* (5), 704−716.
(10) Park, S.; Park, J. M.; Kim, S.; Kim, J.-A.; Shepherd, J. D.; Smith-Hicks, C. L.; Chowdhury, S.; Kaufmann, W.; Kuhl, D.; Ryazanov, A. G.; Huganir, R. L.; Linden, D. J.; Worley, P. F. Elongation Factor 2 and Fragile X Mental Retardation Protein Control the Dynamic Translation of Arc/Arg3.1 Essential for MGluR-LTD. *Neuron* **2008**, *59* (1), 70−83.
(11) Fromer, M.; Pocklington, A. J.; Kavanagh, D. H.; Williams, H. J.; Dwyer, S.; Gormley, P.; Georgieva, L.; Rees, E.; Palta, P.; Ruderfer, D. M.; Carrera, N.; Humphreys, I.; Johnson, J. S.; Roussos, P.; Barker, D. D.; Banks, E.; Milanova, V.; Grant, S. G.; Hannon, E.; Rose, S. A.; Chambert, K.; Mahajan, M.; Scolnick, E. M.; Moran, J. L.; Kirov, G.; Palotie, A.; McCarroll, S. A.; Holmans, P.; Sklar, P.; Owen, M. J.; Purcell, S. M.; O'Donovan, M. C. De Novo Mutations in Schizophrenia Implicate Synaptic Networks. *Nature* **2014**, *506* (7487), 179−184.
(12) Pastuzyn, E. D.; Day, C. E.; Kearns, R. B.; Kyrke-Smith, M.; Taibi, A. V.; McCormick, J.; Yoder, N.; Belnap, D. M.; Erlendsson, S.; Morado, D. R.; Briggs, J. A. G.; Feschotte, C.; Shepherd, J. D. The Neuronal Gene Arc Encodes a Repurposed Retrotransposon Gag Protein That Mediates Intercellular RNA Transfer. *Cell* **2018**, *172* (1−2), 275−288.e18.
(13) Sumner, C.; Ono, A. The "Basics" of HIV-1 Assembly. *PLoS Pathog* **2024**, *20* (2), No. e1011937.
(14) Waheed, A. A.; Freed, E. O. HIV Type 1 Gag as a Target for Antiviral Therapy. *AIDS Res. Hum. Retroviruses* **2012**, *28* (1), 54−75.
(15) Burniston, M. T.; Cimarelli, A.; Colgan, J.; Curtis, S. P.; Luban, J. Human Immunodeficiency Virus Type 1 Gag Polyprotein Multimerization Requires the Nucleocapsid Domain and RNA and Is Promoted by the Capsid-Dimer Interface and the Basic Region of Matrix Protein. *J. Virol* **1999**, *73* (10), 8527−8540.
(16) De Guzman, R. N.; Wu, Z. R.; Stalling, C. C.; Pappalardo, L.; Borer, P. N.; Summers, M. F. Structure of the HIV-1 Nucleocapsid Protein Bound to the SL3 Psi-RNA Recognition Element. *Science* **1998**, *279* (5349), 384−388.
(17) Carlson, L.-A.; Bai, Y.; Keane, S. C.; Doudna, J. A.; Hurley, J. H. Reconstitution of Selective HIV-1 RNA Packaging in Vitro by Membrane-Bound Gag Assemblies. *Elife* **2016**, *5*, DOI: 10.7554/eLife.14663.
(18) Nielsen, L. D.; Pedersen, C. P.; Erlendsson, S.; Teilum, K. The Capsid Domain of Arc Changes Its Oligomerization Propensity through Direct Interaction with the NMDA Receptor. *Structure* **2019**, *27* (7), 1071−1081.e5.
(19) Eriksen, M. S.; Nikolaienko, O.; Hallin, E. I.; Grødem, S.; Bustad, H. J.; Flydal, M. I.; Merski, I.; Hosokawa, T.; Lascu, D.; Akerkar, S.; Cuéllar, J.; Chambers, J. J.; O'Connell, R.; Muruganandam, G.; Loris, R.; Touma, C.; Kanhema, T.; Hayashi, Y.; Stratton, M. M.; Valpuesta, J. M.; Kursula, P.; Martinez, A.; Bramham, C. R. Arc Self-association and Formation of Virus-like Capsids Are Mediated by an N-terminal Helical Coil Motif. *FEBS J.* **2021**, *288* (9), 2930−2955.
(20) Gote, V.; Bolla, P. K.; Kommineni, N.; Butreddy, A.; Nukala, P. K.; Palakurthi, S. S.; Khan, W. A Comprehensive Review of MRNA Vaccines. *Int. J. Mol. Sci.* **2023**, *24* (3), 2700.
(21) Mignone, F.; Gissi, C.; Liuni, S.; Pesole, G. Untranslated Regions of MRNAs. *Genome Biol.* **2002**, *3* (3), No. reviews0004.1.
(22) Amarasinghe, G. K.; De Guzman, R. N.; Turner, R. B.; Chancellor, K. J.; Wu, Z. R.; Summers, M. F. NMR Structure of the HIV-1 Nucleocapsid Protein Bound to Stem-Loop SL2 of the Ψ-RNA Packaging Signal. Implications for Genome Recognition 1 1Edited by P. Wright. *J. Mol. Biol.* **2000**, *301* (2), 491−511.
(23) Webb, J. A.; Jones, C. P.; Parent, L. J.; Rouzina, I.; Musier-Forsyth, K. Distinct Binding Interactions of HIV-1 Gag to Psi and Non-Psi RNAs: Implications for Viral Genomic RNA Packaging. *RNA* **2013**, *19* (8), 1078−1088.
(24) Guo, C.; Yao, X.; Wang, K.; Wang, J.; Wang, Y. Comparison of HIV-1 Gag and NCp7 in Their Selectivity for Package Signal, Affinity for Stem-Loop 3, and Zn2+ Content. *Biochimie* **2020**, *179*, 135−145.
(25) Ashley, J.; Cordy, B.; Lucia, D.; Fradkin, L. G.; Budnik, V.; Thomson, T. Retrovirus-like Gag Protein Arc1 Binds RNA and Traffics across Synaptic Boutons. *Cell* **2018**, *172* (1−2), 262−274.
(26) Segel, M.; Lash, B.; Song, J.; Ladha, A.; Liu, C. C.; Jin, X.; Mekhedov, S. L.; Macrae, R. K.; Koonin, E. V.; Zhang, F. Mammalian Retrovirus-like Protein PEG10 Packages Its Own MRNA and Can Be Pseudotyped for MRNA Delivery. *Science (1979)* **2021**, *373* (6557), 882−889.
(27) Gu, W.; Luozhong, S.; Cai, S.; Londhe, K.; Elkasri, N.; Hawkins, R.; Yuan, Z.; Su-Greene, K.; Yin, Y.; Cruz, M.; Chang, Y.-W.; McMullen, P.; Wu, C.; Seo, C.; Guru, A.; Gao, W.; Sarmiento, T.; Schaffer, C.; Nishimura, N.; Cerione, R.; Yu, Q.; Warden, M.; Langer, R.; Jiang, S. Extracellular Vesicles Incorporating Retrovirus-like Capsids for the Enhanced Packaging and Systemic Delivery of MRNA into Neurons. *Nat. Biomed Eng.* **2024**, *8* (4), 415−426.
(28) Jumper, J.; Evans, R.; Pritzel, A.; Green, T.; Figurnov, M.; Ronneberger, O.; Tunyasuvunakool, K.; Bates, R.; Žídek, A.; Potapenko, A.; Bridgland, A.; Meyer, C.; Kohl, S. A. A.; Ballard, A. J.; Cowie, A.; Romera-Paredes, B.; Nikolov, S.; Jain, R.; Adler, J.; Back, T.; Petersen, S.; Reiman, D.; Clancy, E.; Zielinski, M.; Steinegger, M.; Pacholska, M.; Berghammer, T.; Bodenstein, S.; Silver, D.; Vinyals, O.; Senior, A. W.; Kavukcuoglu, K.; Kohli, P.; Hassabis, D. Highly Accurate Protein Structure Prediction with AlphaFold. *Nature* **2021**, *596* (7873), 583−589.
(29) Mirdita, M.; Schütze, K.; Moriwaki, Y.; Heo, L.; Ovchinnikov, S.; Steinegger, M. ColabFold: Making Protein Folding Accessible to All. *Nat. Methods* **2022**, *19* (6), 679−682.
(30) Ono, A.; Freed, E. O. Plasma Membrane Rafts Play a Critical Role in HIV-1 Assembly and Release. *Proc. Natl. Acad. Sci. U. S. A.* **2001**, *98* (24), 13925−13930.
(31) Sumner, C.; Ono, A. Relationship between HIV-1 Gag Multimerization and Membrane Binding. *Viruses* **2022**, *14* (3), 622.
(32) Ono, A. HIV-1 Assembly at the Plasma Membrane: Gag Trafficking and Localization. *Future Virol* **2009**, *4* (3), 241−257.
(33) Zhang, J. Interplay between Host TRNAs and HIV-1: A Structural Perspective. *Viruses* **2021**, *13* (9), 1819.
(34) Bou-Nader, C.; Muecksch, F.; Brown, J. B.; Gordon, J. M.; York, A.; Peng, C.; Ghirlando, R.; Summers, M. F.; Bieniasz, P. D.; Zhang, J. HIV-1 Matrix-TRNA Complex Structure Reveals Basis for Host Control of Gag Localization. *Cell Host Microbe* **2021**, *29* (9), 1421−1436.e7.
(35) Myrum, C.; Baumann, A.; Bustad, H. J.; Flydal, M. I.; Mariaule, V.; Alvira, S.; Cuéllar, J.; Haavik, J.; Soulé, J.; Valpuesta, J. M.; Márquez, J. A.; Martinez, A.; Bramham, C. R. Arc Is a Flexible Modular Protein Capable of Reversible Self-Oligomerization. *Biochem. J.* **2015**, *468* (1), 145−158.
(36) Guth-Metzler, R.; Mohamed, A. M.; Cowan, E. T.; Henning, A.; Ito, C.; Frenkel-Pinter, M.; Wartell, R. M.; Glass, J. B.; Williams, L. D. Goldilocks and RNA: Where Mg2+ Concentration Is Just Right. *Nucleic Acids Res.* **2023**, *51* (8), 3529−3539.
(37) Yamagami, R.; Sieg, J. P.; Bevilacqua, P. C. Functional Roles of Chelated Magnesium Ions in RNA Folding and Function. *Biochemistry* **2021**, *60* (31), 2374−2386.
(38) Misra, V. K.; Draper, D. E. The Linkage between Magnesium Binding and RNA Folding 1 1Edited by B. Honig. *J. Mol. Biol.* **2002**, *317* (4), 507−521.

(39) Gruber, A. R.; Lorenz, R.; Bernhart, S. H.; Neuböck, R.; Hofacker, I. L. The Vienna RNA Websuite. *Nucleic Acids Res.* **2008**, *36* (WebServer issue), W70−W74.
(40) Xue, C. S.; Erika, G.; Jiří, H. Surface Plasmon Resonance Biosensor for the Ultrasensitive Detection of Bisphenol A. *Anal Bioanal Chem* **2019**, *411* (22), 5655−5658.
(41) Vaisocherová, H.; Zhang, Z.; Yang, W.; Cao, Z.; Cheng, G.; Taylor, A. D.; Piliarik, M.; Homola, J.; Jiang, S. Functionalizable Surface Platform with Reduced Nonspecific Protein Adsorption from Full Blood Plasma−Material Selection and Protein Immobilization Optimization. *Biosens Bioelectron* **2009**, *24* (7), 1924−1930.

https://doi.org/10.1021/acs.langmuir.4c03151
Langmuir 2024, 40, 23473−23482